Electron Impact Fragmentations of Chlorinated Organophosphorus Pesticides

Jongki Hong,* Do-Gyun Kim, and Ki-Jung Paeng†

Korea Basic Science Institute, 52 Eoun-Dong, Yusung-Ku, Taejeon 305-333, Korea
†Department of Chemistry, Yonsei University, Wonju 220-710, Korea
Received April 19, 2000

Mass spectral fragmentations of six chlorinated organophosphorus pesticides were investigated using electron impact mass spectrometry. Understanding the fragmentation pathways, based on the fragment ions of mass spectra, should be useful in the structural elucidation and chemical identification of these compounds. The proposed fragmentation pathways were verified by collision-induced dissociation B/E-linked scan spectra. In most cases, the structures of characteristic fragment ions could be expected by the observation of the peak clusters due to ^{35}Cl and ^{37}Cl isotopes. According to substituted groups on phosphorus atom, phosphate and phosphorothioate exhibited significantly different fragmentation patterns. Especially, phosphate and phosphorothioate with diethyl ester produced more diverse fragment ions than that with dimethyl ester.

Introduction

The importance of mass spectrometry for pesticide chemistry, particular for the identification of small quantities encountered in environmental residue, has been recognized.[1-3] Mass spectrometry of pesticides, using a variety of ionization techniques such as electron impact (EI), chemical ionization (CI) and fast atom bombardment (FAB) has been intensively studied.[4-6] Especially, EI method has been popularly used for the determination of pesticides in a various environmental samples due to its easy combination with gas chromatography and to an excellent sensitivity. Moreover, EI mass spectral method provides structurally important information of pesticides and their environmental metabolites. However, in the case of mass spectral fragmentation studies, the reliability of fragmentation pathways and their mechanisms based on the ordinary mass spectrometric method is doubtful. Thus, several tandem mass spectrometric methods such as daughter ion scan, parent ion scan, neutral loss scan and selected reaction monitoring are necessary for the identification of pesticides.[7,8] Each method has its own advantage, particularly for the structural identification of a class of compounds by characteristic reactions.[9]

Although mass fragmentation patterns of organophosphorus pesticides have been intensively studied according to phosphorus groups such as phosphates, phosphorothioates and phosphorusdithioates,[10-12] the fragmentation processes and mechanisms for chlorinated organophosphorus pesticides have not been studied in detail. We have been interested in the structural determination of chlorinated organophosphorus pesticides under EI mode because of their importance in environmental and agricultural aspects. The information obtained is useful for the determination of chlorinated phosphorus pesticides in environmental samples.

*Author to whom correspondence should be addressed at Mass Spectrometry Team, Korea Basic Science Institute, 52 Eoun-Dong, Yusung-Ku, Taejeon 305-333, Korea, Tel: +82-42-865-3430; Fax: +82-42-865-3419; E-mail: jongki@comp.kbsi.re.kr

We studied the general fragmentation processes of chlorinated organophosphorus pesticides using EI mode. Moreover, the mechanisms of the fragmentations for chlorinated organophosphorus pesticides have been elucidated using collision-induced dissociation (CID) B/E-linked scan technique.

Experimental Section

Six chlorinated organophosphorus pesticides were purchased from Dr. Ehrenstrofer (Germany) and Chem Service (U. S. A.) with 97-99% purity and used without any further purification. All solvents were HPLC grade and purchased from J. T. Baker (Phillisburg, NJ, U. S. A.).

Mass spectra were recorded on a JEOL SX-102A double focusing instrument (JEOL Ltd., Akishima, Japan) with BE reverse geometry using direct probe insertion which could be operated at temperatures varying between 30 and 200 °C. The temperature of ion source was maintained at 180 °C. The compounds were ionized by 70 eV electron energy and accelerated to 10 kV. The products ions generated by collision-induced dissociation (CID) in the first field-free region of the instrument were analyzed using linked scanning at constant B/E ratio. The collision gas (helium) pressure was adjusted for a 50% attenuation of the primary ion beam. The mass scan range was between 0 and 400 amu every 12 sec.

Results and Discussion

The EI-mass spectra of six chlorinated organophosphorus pesticides studied are shown in Figure 1. Mass spectra of chlorinated organophosphorus pesticides can be characterized by the presence of isotopic distributions in fragment ions from ^{37}Cl and ^{34}S and the presence of common fragment ions produced from organophosphorus moiety under EI mode. The pathways for the production of fragments with organophosphorus moiety are shown in Scheme 1. For phosphorus moiety with dimethylester, characteristic ions are generated by the successive losses of formaldehydes via

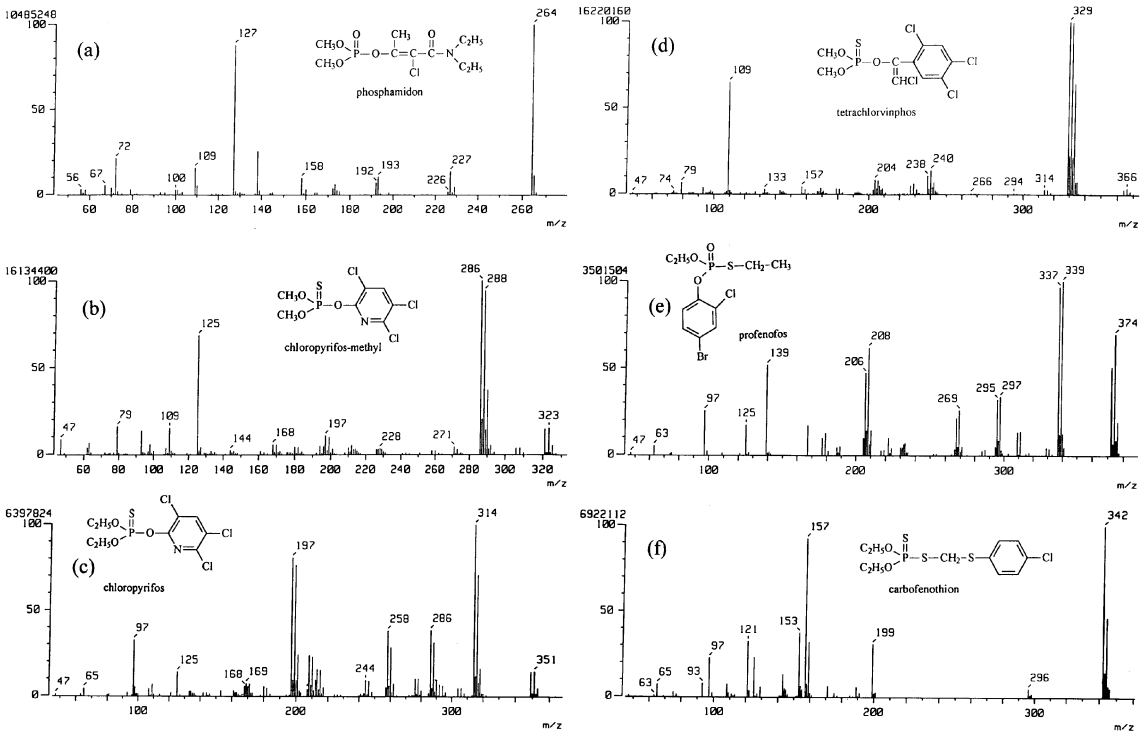

Figure 1. EI mass spectra of six chlorinated organophosphorus pesticides: (a) phosphamidon, (b) chloropyrifos-methyl, (c) chloropyrifos, (d) tetrachlorvinphos, (e) profenofos, and (f) carbofenothion.

A. In the case of dimethyl phosphate or phosphorothioate

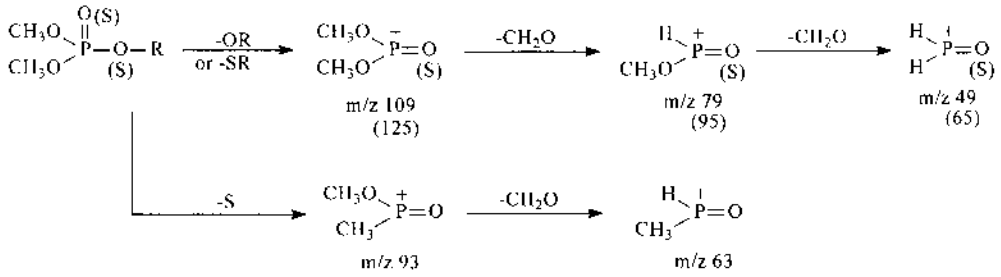

B. In the case of diethyl phosphate or phosphorothioate

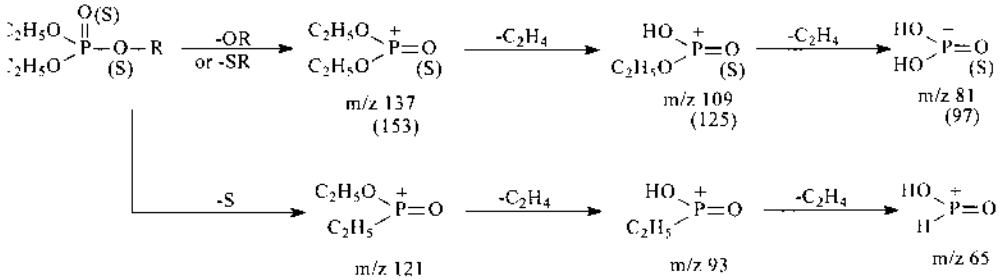

Scheme 1. Basic fragmentation patterns of dimethyl and diethyl phosphate moiety.

four-centered transition state. On the other hand, characteristic ions of phosphorus moiety with diethylester are formed by the successive elimination of ethene molecules through four-centered transition state. Moreover, the relative abundance of ions (m/z 153, 137, 125, 109, 93 and 79) indicative of organophosphorus moiety is influenced by the substituents on organophosphorus group, as shown in Figure 1. To further confirm the fragmentation pathways, CID B/E-linked

Table 1. CID B/E-linked scan spectra of product ions for phosphamidon

Precursor ion (m/z)	R.A. (%)	Product ion (m/z)	R.A. (%)
264 $[M\text{-}Cl]^+$	100	247 $[P\text{-}OH]^+$	23
		193 $[P\text{-}NC_4H_9]^+$	21
		138 $[P\text{-}(CH_3O)_2P(OH)_2]^+$	32
		127 $[(CH_3O)_2P(OH)_2]^-$	15
227 $[M\text{-}N(C_2H_5)_2]^+$	100	199 $[PCO]^-$	10
		192 $[P\text{-}Cl]^-$	37
193 $[M\text{-}Cl\text{-}NC_4H_9]^-$	100	178 $[P\text{-}CH_3]^-$	10
		164 $[P\text{-}CH_2O\text{-}H]^-$	13
		127 $[(CH_3O)_2P(OH)_2]^-$	38
138 $[M\text{-}Cl\text{-}(CH_3O)_2P(OH)_2]^-$	100	110 $[P\text{-}C_2H_4]^+$	17
		72 $[N(C_2H_5)]^-$	21
		67 $[P\text{-}NC_4H_9]^+$	24
127 $[(CH_3O)_2P(OH)_2]^-$	100	109 $[P\text{-}H_2O]^-$	14
		95 $[P\text{-}CH_3\text{-}OH]^-$	11
100 $[OCN(C_4H_{10})]^+$	100	72 $[P\text{-}CO]^-$	16

R.A.: relative abundance.

scan was performed on the major fragments present in the EI spectra. Tables 1 to 7 show the product ions observed in the CID spectra of molecular ions as well as typical fragment ions. On the basis of CID B/E linked scan spectra, the fragmentation pathways are suggested as shown in Schemes 2 to 8. Fragmentations of these compounds typically produce characteristic spectra by rearrangements and cleavage when the precursor ions are analyzed by CID-B/E linked scan.

Phosphamidon. As shown in Figure 1(a), the molecular ion is not shown because of the easy of Cl radical fragmentation whileas $[M\text{-}Cl]^+$ ion at m/z 264 is appeared as base peak. The formation of other significant fragment ions is suggested in Scheme 2, on the basis of B/E-linked scan spectra data (Table 1). The ion at m/z 264 shows the diverse fragmentation through resonance structure, as shown in Scheme 2. The CID B/E-linked scan spectrum of m/z 264 shows the characteristic product ions at m/z 247, 193, 138, and 127. The product ion at m/z 247 is formed by the loss of OH radical from the precursor ion m/z 264 but this ion is not observed in EI-spectrum. The losses of NC_4H_9 radical and dimethylphophoric acid from the precursor ion of m/z 264 yield the product ions at m/z 193 and 138, respectively. The significantly abundant ion at m/z 127 is expected to be $[(CH_3O)_2P(OH)_2]^+$ ion. This ion may be generated by double hydrogen rearrangement from the substituted vinyl methane and ethane group to phosphorus oxygen. This ion has been also observed in deuterium labeled-methane chemical ionization mode.[13] The loss of $N(C_2H_5)_2$ radical from molecular ion gives the fragment ion cluster at m/z 227 and 229 to form terminus carbonyl ion. However, the fragment ion at m/z 199 formed by the loss of CO molecule from the ion at 227 is not observed probably due to the presence of electron withdrawing Cl atom. The ion at m/z 100 corresponding to N,N-diethyl isocyanate ion has a very weak intensity peak whereas the ion at m/z 72 which is formed by the loss of CO molecule from diethyl isocyanate ion through inductive cleavage appears as relatively abundant ion. Typical fragmentations of dimethyl phosphate moiety produce the characteristic ions at m/z 109 and 79.

Chloropyrifos-methyl. Chloropyrifos-methyl gives the molecular ion cluster at m/z 321 and 323 and the base peak

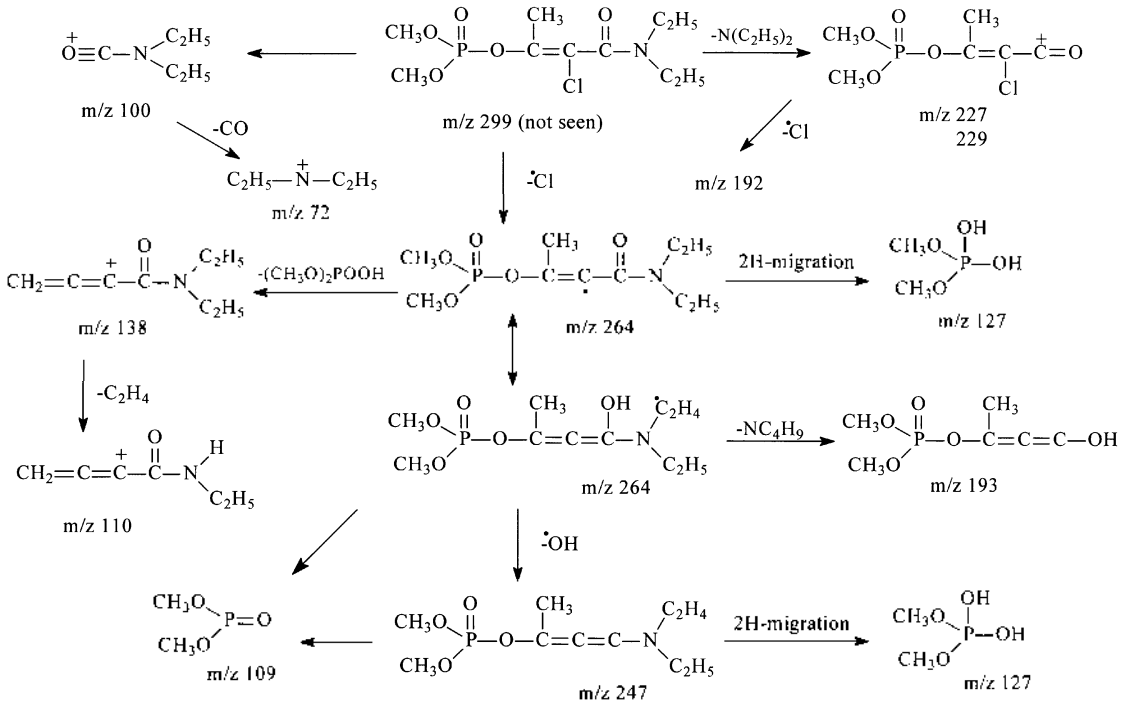

Scheme 2. Mass spectral fragmentation pathways of phosphamidon.

Table 2. CID B/E-linked scan spectra of product ions for chloropyrifos-methyl

Precursor ion (m/z)	R.A. (%)	Product ion (m/z)	R.A. (%)
321 $[M]^+$	100	306 $[M\text{-}CH_3]^+$	22
		286 $[M\text{-}Cl]^+$	92
		197 [trichloropyriol]$^-$	10
		180 [trichloropyriol-OH]$^-$	12
		125 $[(CH_3O)_2P{=}S]^+$	54
		109 $[(CH_3O)_2P{=}O]^+$	28
		93 $[(CH_3O)(CH_3)P{=}S]^+$	21
286 $[M\text{-}Cl]^+$	100	271 $[P\text{-}CH_3]^+$	18
		224 $[P\text{-}CH_2O\text{-}S]^-$	13
		208 $[P\text{-}(CH_3O)_2\text{-}S{+}O]^-$	14
		125 $[(CH_3O)_2P{=}S]^+$	18
		109 $[(CH_3O)_2P{=}O]^+$	20
		93 $[(CH_3O)(CH_3)P{=}S]^+$	45
197 [trichloropyriol]$^+$	100	180 $[P\text{-}OH]^+$	28
		168 $[P\text{-}CHO]^-$	22
		134 $[P\text{-}CO\text{-}Cl]^-$	13
		107 $[P\text{-}C_2H_2NOCl]^+$	38

R.A.: relative abundance.

ion cluster at m/z 286, 288 and 290, as shown in Figure 1(b). The CID B/E-linked scan spectral data for the characteristic ions of chloropyrifos-methyl are summarized in Table 2. The suggested fragmentation pathways of chloropyrifos-methyl are shown in Scheme 3. The fragment ions at m/z 286 and 306 are formed by the consecutive loss of Cl and CH_3 radicals from molecular ion, respectively. However, the fragment ions lost formaldehyde molecule from M^+ and $[M\text{-}Cl]^+$ ions are not produced, as shown in Table 2. The CID B/E-linked scan spectrum of precursor ion at m/z 286 exhibits diverse fragment ions at m/z 271 (by the loss of CH_3 radical), 224 (by the losses of CH_2O and S atom) and 109. However, the product ion at m/z 224 is not observed in EI mass spectrum of chloropyrifos-methyl. The ion cluster (m/z 197, 199 and 201) can be assigned trichloropyriol ion which is formed through γ-hydrogen rearrangement. The CID B/E-linked scan spectrum of the ion at m/z 197 produces the product ions at m/z 180 and 168 which are generated by the losses of OH and CHO radical, respectively. These product ions are also observed in the CID B/E-linked scan spectrum of the ion at m/z 197 for chloropyrifos. In addition, the characteristic ions of dimethyl phosphorothioate moiety, at m/z 125, 109 and 93 are also observed in EI-mass spectrum of chloropyrifos.

Chloropyrifos. The chemical structure of chloropyrifos is very similar to that of chloropyrifos-methyl, while its fragmentation pattern is significantly different from that of latter, as shown in Figure 1(b) and (c). The fragmentation pathways are depicted in Scheme 4. The base peak is appeared the ion at m/z 314 by the loss of Cl radical from molecular ion. The significantly abundant ions at m/z 286 and 258 are formed by the successive elimination of ethene molecules from $[M\text{-}Cl]^+$ ion. The product ion at m/z 208 may be formed by the concerted losses of OC_2H_5 radical and S atom from the ion at m/z 286. Unfortunately, the formation mechanism of this ion can not be clearly explained at the moment. Particularly, the loss of OC_2H_5 radical from molecular ion produces the ion at m/z 304. The fragment ion at m/z 276 is produced by the loss of ethene molecule from the ion m/z 304. Subsequent loss of S atom may yield the fragment ion

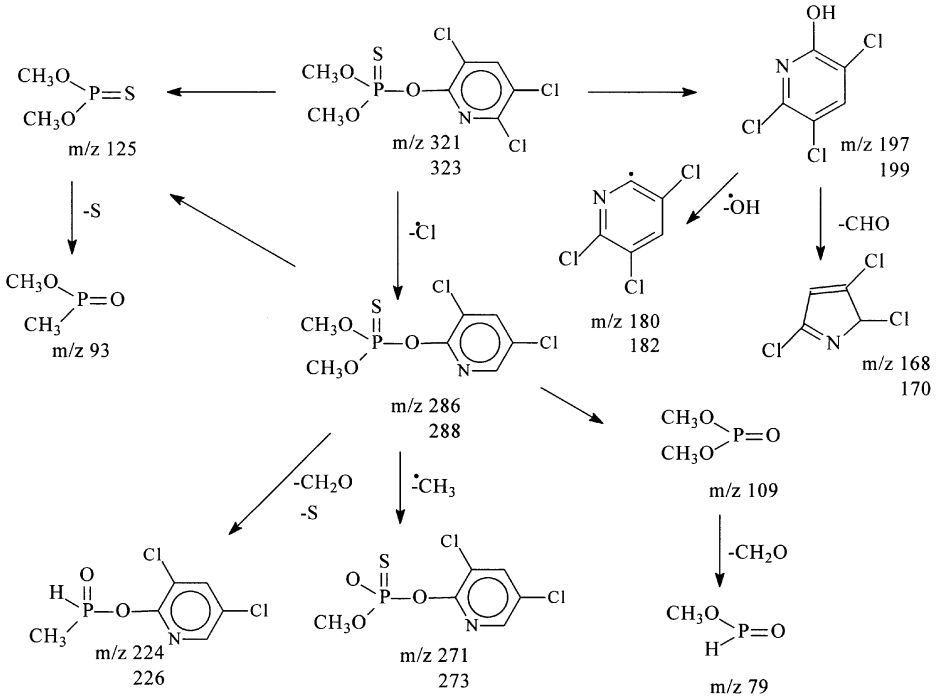

Scheme 3. Mass spectral fragmentation pathways of chloropyrifos-methyl.

Table 3. CID B/E-linked scan spectra of product ions for chloropyrifos

Precursor ion (m/z)	R.A. (%)	Product ion (m/z)	R.A. (%)
349 $[M]^+$	100	314 $[M-Cl]^+$	92
		286 $[M-Cl-C_2H_4]^-$	52
		276 $[M-(C_2H_4)_2-OH]^+$	21
		258 $[M-Cl-(C_2H_4)_2]^-$	43
		208 $[M-Cl-(C_2H_5O)_2\ S+O]^-$	31
		197 [trichloropyriol]$^-$	19
314 $[M-Cl]^-$	100	286 $[P-C_2H_4]^+$	74
		258 $[P-(C_2H_4)_2]^+$	26
		208 $[P-(C_2H_5O)_2-S-O]^+$	17
		190 [1-ethoxy, 2,4-dichloropyridine]$^-$	20
		125 $[P-(C_2H_5O)(OH)P=S]^+$	22
		93 $[P-(C_2H_5)(OH)P=O]^-$	25
		65 $[P-(OH)(H)P=O]^-$	23
304 $[M-OC_2H_5]^+$	100	276 $[P-C_2H_4]^+$	35
		244 $[P-C_2H_4-S]^+$	24
		241 $[P-Cl]^-$	16
286 $[M-Cl-C_2H_4]^+$	100	258 $[P-C_2H_4]^+$	63
		208 $[P-OC_2H_5-OH-S-O]^+$	13
		190 [1-ethoxy, 2,4-dichloropyridine]$^-$	10
197 [trichloropyriol]$^+$	100	180 $[P-OH]^+$	32
		168 $[P-CHO]^+$	22
		134 $[P-CO-Cl]^+$	13
		107 $[P-C_2H_2NOCl]^+$	38
153 $[(C_2H_5O)_2P(S)]^+$	100	125 $[P-C_2H_4]^+$	53
		121 $[P-S]^+$	22
		97 $[P-2C_2H_4]^+$	18

R.A.: relative abundance.

at m/z 244. The trichloropyriol ion, also appeared with low intensity in the mass spectrum of chloropyrifos-methyl, exhibits prominently in this mass spectrum. It can be explained that trichloropyriol from chloropyrifos is formed by hydrogen migration from diethyl group to oxygen atom attached to benzene ring *via* sterically favorable six-membered cyclic transition state whereas that from chloropyrifos-methyl is generated by hydrogen migration from dimethyl group to oxygen through four-centered cyclic transition state. Furthermore, fragmentations of diethyl phosphorothioate moiety yield the characteristic ions at m/z 125 and 97 but do not produce other characteristic ions at m/z 153 and 121.

Tetrachlorvinphos. Tetrachlorvinphos yields a weak molecular ion due to easy loss of Cl radical and produces a few significant fragments, as shown in Figure 1(d). The base peak at m/z 329 is formed by the loss of Cl radical from molecular ion and consecutive loss of Cl radical yields the product ion at m/z 294 to form rigid side ring on benzene group, as depicted in Scheme 5. The ion cluster at m/z 238 and 240 must be arisen *via* the elimination of phosphoric acid from molecular ion, accompanied with hydrogen transfer from the ethylene moiety. As shown in Table 4, the characteristic ion at m/z 204 from the ion at m/z 238 may be formed by the substitution of Cl by H. The consecutive elimination of HCl and Cl radical from the ion at m/z 204 leads to the fragment ions at m/z 168 and 133, respectively. Characteristic ions of dimethyl phosphorothioate moiety are also abundantly observed at m/z 109 and 79 but another characteristic ion at m/z 125 is not observed.

Profenofos. As seen in Figure 1(e), profenofos gives a strong molecular ion cluster and several characteristic ions

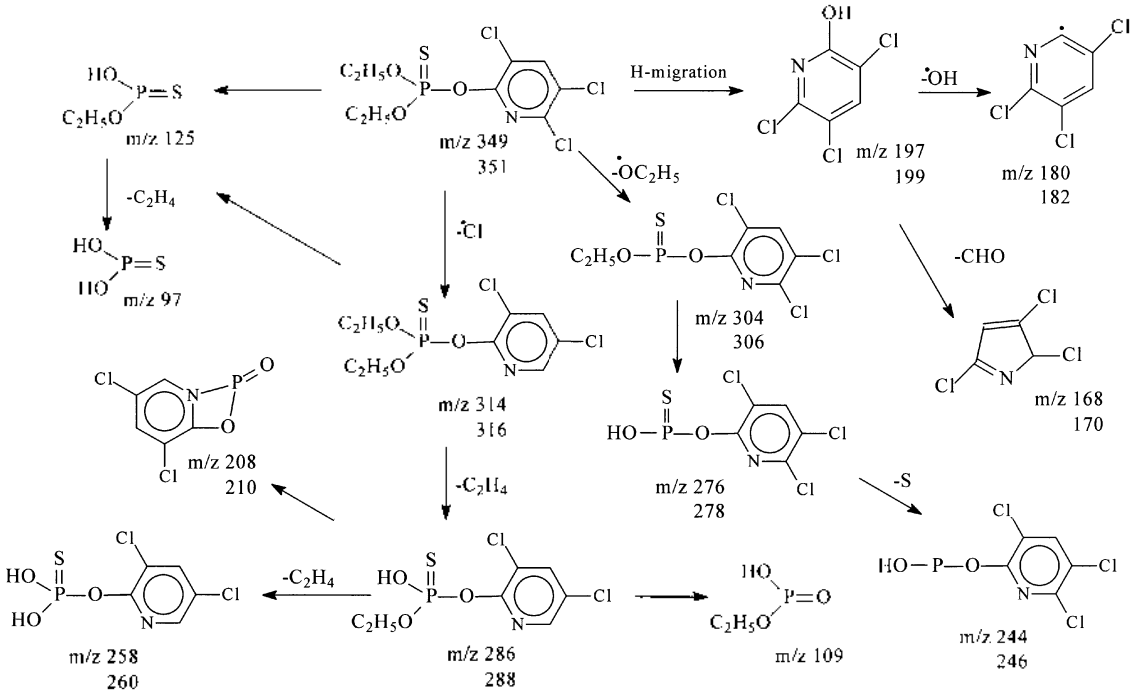

Scheme 4. Mass spectral fragmentation pathways of chloropyrifos.

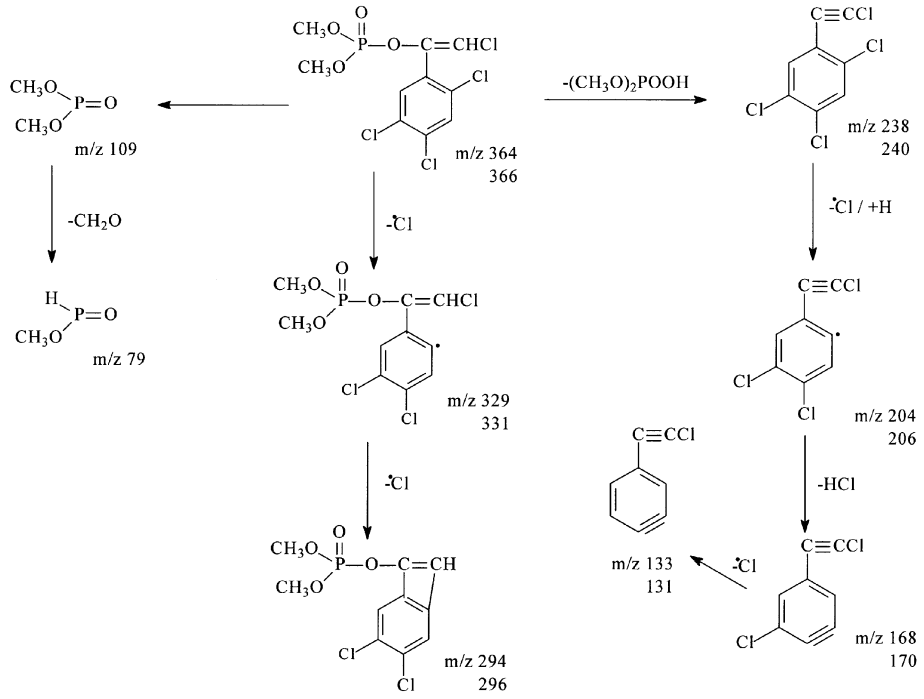

Scheme 5. Mass spectral fragmentation pathways of tetrachlorvinphos.

Table 4. CID B/E-linked scan spectra of product ions for tetrachlorvinphos

Precursor ion (m/z)	R.A. (%)	Product ion (m/z)	R.A. (%)
364 $[M]^-$	100	329 $[M\text{-}Cl]^-$	95
		238 $[M\text{-}(CH_3O)_2POOH]^-$	28
		204 $[M\text{-}Cl\text{-}(CH_3O)_2PO_2]^-$	30
		109 $[(CH_3O)_2P{=}O]^+$	75
		79 $[(CH_3O)(H)P{=}O]^-$	28
329 $[M\text{-}Cl]^+$	100	294 $[P\text{-}Cl]^-$	18
		109 $[(CH_3O)_2P{=}O]^+$	42
		79 $[(CH_3O)(H)P{=}O]^-$	22
238 $[M\text{-}(CH_3O)_2POOH]^-$	100	204 $[P\text{-}CH]^+$	35
		168 $[P\text{-}Cl_2]^-$	26
		133 $[P\text{-}Cl_2\text{-}Cl]^+$	32
		98 $[P\text{-}Cl_4]^-$	24

R.A.: relative abundance.

are produced in its mass spectrum because of the presence of phosphorothioate group containing the chlorine and bromine substituted on benzene ring. Most of the ions containing the aromatic ring are of significant intensity due to a stable aromatic system. The fragmentation pathways of profenofos are depicted in Scheme 6. The CID B/E-linked scan spectral data are summarized in Table 5. The abundant ion at m/z 339 is due to the ^{81}Br isotopic peak of m/z 337 ion which is formed by the loss of Cl radical from molecular ion. As shown in Scheme 6 and Table 5, a various product ions of m/z 337 by CID B/E-linked scan is generated. The product ions at m/z 309, 295 and 234 are formed by the loss of C_2H_4, C_3H_6 and $[SC_3H_6 + C_2H_4]^-$ ion, respectively. The fragment ion at m/z 267 is formed by the elimination of C_3H_6 radical and C_2H_4 molecule from the ions at m/z 309 and 295, respectively. The ions at m/z 167 and 139 having no halogen isotopic peak are generated from the fragmentation of molecular ion, since they are not observed in the CID B/E-linked scan spectra of other characteristic ions, as can be seen in Table 5. The dominant ion cluster at m/z 206 and 208 can be assigned as 2-chloro, 4-bromophenol ion, based on the isotopic analysis. This ion produces a characteristic ion cluster at m/z 177 and 179 eliminating CHO radical in the CID B/E-linked scan mode. The fragment ions at m/z 125 and 97 as the characteristic ions of ethyl phosphorothioate group are also observed.

Carbofenothion. The molecular ion is observed as base peak, as shown in Figure 1(f). The fragmentation pathways of carbofenothion are depicted in Scheme 7, based on the CID B/E-linked scan spectral data (Table 6). The fragment ion cluster at m/z 296 and 298 with low abundance is formed by the elimination of $CH_2{=}S$ *via* four-centered transition state. The fragment ion at m/z 199 is produced by the loss of SPhCl radical from molecular ion through the α-cleavage with charge retention on the sulfur atom attached to phosphorus atom, and successive losses of C_2H_4 molecules yield the product ions at m/z 171 and 143. The abundant ion cluster at m/z 157 and 159 may be formed by the α-cleavage with charge retention on the sulfur atom attached to benzene ring. The fragment ion at m/z 121 is originated from the loss of Cl radical from the ion at m/z 157. The characteristic ions of diethyl phosphorodithioate moiety such as the fragment ions at m/z 153, 125, 121, 105, 97, 93, and 65 are appeared by the consecutive elimination of C_2H_4 molecules, the removal of oxygen and sulfur atoms, as shown in Scheme 7. In particular, the conversion of the ion at m/z 153 to the ion at m/z 121 through the removal of

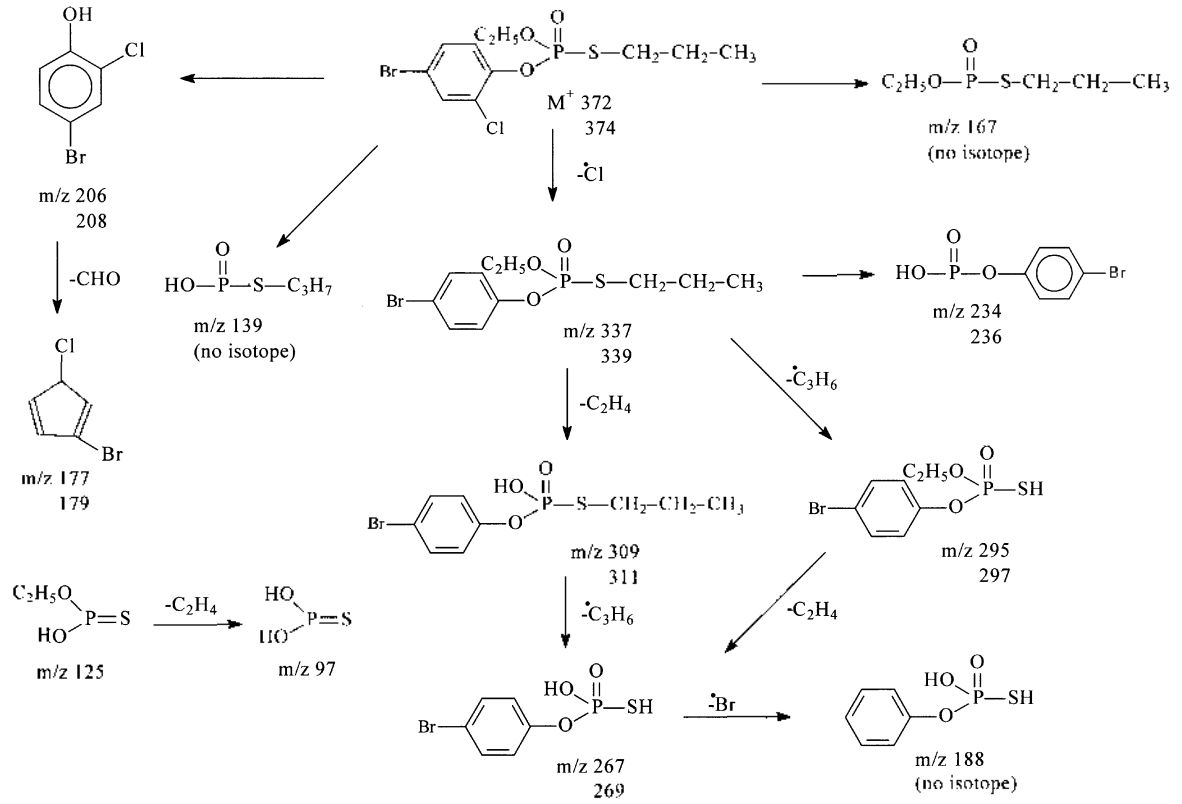

Scheme 6. Mass spectral fragmentation pathways of profenofos.

Table 5. CID B/E-linked scan spectra of product ions for profenofos

Precursor ion (m/z)	R.A. (%)	Product ion (m/z)	R.A. (%)
372 $[M]^+$	100	337 $[P\text{-}Cl]^+$	68
		295 $[M\text{-}Cl\text{-}C_3H_6]^+$	18
		267 $[M\text{-}Cl\text{-}C_3H_6\text{-}C_2H_4]^-$	16
		206 [2-chloro, 4-bromophenol]$^-$	38
		167 $[M\text{-}OC_6H_3BrCl]^-$	34
		139 $[M\text{-}C_2H_4\text{-}OC_6H_3BrCl]^+$	12
		97 $[(OH)_2P{=}S]^+$	21
337 $[M\text{-}Cl]^-$	100	309 $[P\text{-}C_2H_4]^+$	26
		295 $[P\text{-}C_3H_6]^+$	20
		267 $[P\text{-}C_2H_4\text{-}C_3H_6]^+$	41
		188 $[P\text{-}C_2H_4\text{-}C_3H_6\text{-}Br]^+$	14
309 $[M\text{-}Cl\text{-}C_2H_4]^+$	100	267 $[P\text{-}C_3H_6]^+$	52
		234 $[P\text{-}SC_3H_7]^-$	20
		188 $[P\text{-}C_3H_6\text{-}Br]^-$	22
295 $[M\text{-}Cl\text{-}C_3H_6]^+$	100	267 $[P\text{-}C_2H_4]^+$	45
		188 $[P\text{-}C_2H_4\text{-}Br]^-$	10
267 $[M\text{-}Cl\text{-}C_2H_4\text{-}C_3H_6]^-$	100	249 $[P\text{-}H_2O]^-$	21
		188 $[P\text{-}Br]^+$	13
206 [2-chloro, 4-bromophenol]$^-$	100	177 $[P\text{-}CHO]^-$	14
		170 $[P\text{-}HCl]^-$	10

R.A.: relative abundance.

sulfur atom and followed by the rearrangement of oxygen is still ambiguous mechanism, even though previously proposed by Pritchard *et al.*[14] In this study, this conversion ion is also observed in the CID B/E-linked scan spectrum of the precursor ion at m/z 153. On the other hand, the product ion at m/z 121 is not observed in the CID B/E-linked scan spectrum of the precursor ion at m/z 153 of chloropyrifos. Moreover, the CID B/E-linked scan spectrum of the precursor ion at m/z 121 (not shown in here) yields the product ions at m/z 93 and 65 due to the successive loss of C_2H_4 molecules.

Conclusion

The mass fragmentation pathways for chlorinated phosphorus pesticides have been suggested on the basis of the spectra obtained from CID B/E-linked scan. The losses of formaldehyde for dimethyl phosphorus moiety and ethene for diethyl phosphorus moiety were commonly observed by rearrangement reactions where hydrogen transfers to the phosphorus to eliminate formaldehyde and to the oxygen to eliminate ethene. However, such rearrangement reactions were not observed in CID B/E-linked scan spectra for molecular ion. For dimethyl phosphorus moiety, the molecular and $[M\text{-}Cl]^+$ ions preferably lost CH_3 radical instead of formaldehyde. For diethyl phosphorus moiety, $[M\text{-}Cl]^+$ ion proceeded the consecutive loss of C_2H_4 molecule to form $[M\text{-}Cl\text{-}C_2H_4]^-$ and $[M\text{-}Cl\text{-}2C_2H_4]^-$ ions, whereas molecular ion produced $[M\text{-}OC_2H_5]^-$ ion. The fragmentation mechanism for these compounds could be extended to interpret the mass spectra of other pesticides.

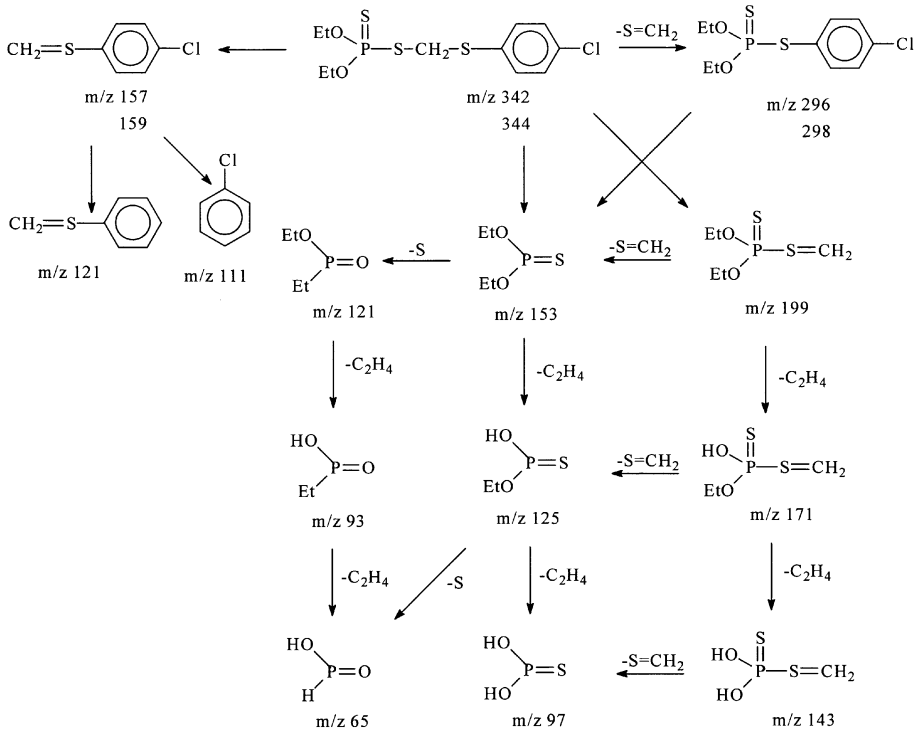

Scheme 7. Mass spectral fragmentation pathways of carbofenothion.

Table 6. CID B/E-linked scan spectra of product ions for carbofenothion

Precursor ion (m/z)	R.A. (%)	Product ion (m/z)	R.A. (%)
342 $[M]^+$	100	296 $[P\text{-}S{=}CH_2]^-$	25
		199 $[(C_2H_5O)_2P(S)SCH_2]^-$	41
		157 $[ClH_2SPhCl]^-$	52
		153 $[(C_2H_5O)_2P{=}S]^+$	32
		121 $[(C_2H_5O)(C_2H_5)P{=}O]^-$	21
		97 $[(OH)_2P{=}S]^-$	18
296 $[M\text{-}S{=}CH_2]^-$	100	153 $[(C_2H_5O)_2P{=}S]^-$	21
		125 $[(HO)(C_2H_5O)P{=}S]^-$	24
199 $[(C_2H_5O)_2P(S)SCH_2]^-$	100	171 $[P\text{-}C_2H_4]^-$	14
		153 $[(C_2H_5O)_2P{=}S]^-$	12
		143 $[P\text{-}(C_2H_5O)_2P{=}S]^-$	13
157 $[CH_2{=}S\text{-}PhCl]^-$	100	121 $[P\text{-}HCl]^+$	21
		111 $[P\text{-}CH_2{=}S]^+$	16
		75 $[C_6H_3]^-$	33
		45 $[CHS]^+$	42
153 $[(C_2H_5O)_2P(S)]^+$	100	125 $[P\text{-}C_2H_4]^+$	24
		97 $[P\text{-}2C_2H_4]^-$	18

R.A.: relative abundance.

References

1. Roach, J. A.; Carson, L. J. *J. Assoc. Off. Anal. Chem.* **1987**, *70*, 439.
2. Hong, J.; Eo, Y.; Rhee, J.; Kim, T.; Kim, K. *J. Chromatogr.* **1993**, *639*, 261.
3. Betowski, L. D.; Jones, T. L. *Environ. Sci. Technol.* **1988**, *22*, 1430.
4. Damico, N. J. *J. Assoc. Off. Anal. Chem.* **1966**, *49*, 1027.
5. Swackamer, D. L.; Charles, J.; Hites, R. A. *Anal. Chem.* **1987**, *59*, 913.
6. Kuivalainen, T.; Kostiainen, R.; Uggla, R.; Sundberg, M. R.; Bjork, H. *J. Am. Soc. Mass Spectrom.* **1996**, *7*, 189.
7. Yost, R. A.; Fetterolf, D. D. *Mass Spectrom. Rev.* **1983**, *2*, 1.
8. Hong, J.; Shin, C.-M.; Kim, Y. H.; Yoo, J. S. *Rapid Commun. Mass Spectrom.* **1999**, *13*, 354.
9. Hummel, S. V.; Yost, R. A. *Org. Mass Spectrom.* **1986**, *21*, 785.
10. Keck, H.; Tommes, P. *J. Mass Spectrom.* **1999**, *34*, 44.
11. Yates, B. F.; Bouma, W. J.; Radom, L. *J. Am. Chem. Soc.* **1984**, *106*, 5805.
12. Zeller, L.; Farrell, Jr. J.; Vainiotalo, P.; Kenttamaa, H. I. *J. Am. Chem. Soc.* **1992**, *114*, 1205.
13. Holmstead, R. L.; Casida, J. E. *J. Off. Anal. Chem.* **1974**, *57*, 1050.
14. Pritchard, J. G. *Org. Mass Spectrom.* **1970**, *3*, 163.